

# Multilayer piezoelectric actuator with AgPd internal electrode

In-Ho Im<sup>a,\*</sup>, Hoy-Seung Chung<sup>a</sup>, Dong-Soo Paik<sup>a</sup>, Chang-Yub Park<sup>a</sup>, Jong-Joo Park<sup>b</sup>,  
Seon-Gi Bae<sup>c</sup>

<sup>a</sup>Department of Electrical Engineering, Yonsei University, 134, Shinchon, Seoul, South Korea

<sup>b</sup>Department of Chemistry, Myonggi University, 38-2, Namdong, Yongin-Si, Kyungki-Do, South Korea

<sup>c</sup>Department of Electrical Engineering, Incheon University, 177, Dowha-don, Icheon, South Korea

Received 3 March 1999; received in revised form 5 August 1999; accepted 10 August 1999

---

## Abstract

Using 70Ag/30Pd paste as an internal electrode which can be sintered at low temperature and have cost down effect in mass productions, multilayer piezoelectric actuators (MPAs) were fabricated with 75 layers, 30  $\mu\text{m}$  thickness layer, by conventional multilayer capacitor (MLC) techniques. The multilayer piezoelectric actuators had no defects such as diffusions of the internal electrode to ceramic body and shortage of internal electrodes. The MPA did not show the cracks in the ceramics parts and the gapping phenomena in the external electrodes when Ag paste was used as external electrodes. The MPA devices showed a maximum displacement of 4  $\mu\text{m}$  at 100 V dc voltage and kept the maximum displacement constant for 300 s. The MPA showed good matching properties between ceramic bodies and AgPd internal electrodes. We confirmed the possibility of large scale production of the multilayer piezoelectric actuators with superior electrical properties and a cost down effect using 70Ag/30Pd paste as an internal electrode. © 2000 Elsevier Science Ltd. All rights reserved.

*Keywords:* Actuators; Ag/Pd; Electrodes; Multilayers; Piezoelectric properties

---

## 1. Introduction

Piezoelectric and electrostrictive materials for actuators are widely used in applications requiring precision displacement control or high generative force, i.e. optical stage, precision mechano-electronics, and semiconductor devices.<sup>1–3</sup> In particular, multilayer piezoelectric actuators (hereafter, MPAs) have been widely studied because the assets of MPAs are a rapid operation, a low power consumption, a high precision control and no noise,<sup>4,5</sup> compared with the electromagnetic actuators. The MPAs with Pd or Pt internal electrodes<sup>6,7</sup> have been investigated to achieve a low driving voltage<sup>8</sup> ( $\leq 1$  kV) and a high reliability. Takahashi et al.<sup>6,7</sup> suggested the possibilities of mass production and low driving voltage ( $< 200$  V) of the MPA made of  $0.65\text{Pb}(\text{Mg}_{1/3}\text{Nb}_{2/3})\text{O}_3$ – $0.35\text{PbTiO}_3$  and reported the effects of the ratio of internal electrode area to cross-sectional area of the MPA to its characteristics.

The manufacturing costs of the MPA devices with 100% Pd or 100% Pt paste as internal electrodes are very high in mass production because pure metal pastes are very expensive. The piezoelectric characteristics of the MPA with 100% Pd internal electrodes were degraded due to the gapping phenomena by thermal expansion coefficient difference between Pd internal electrodes and ceramics parts or protection phenomena by thermal diffusion of Ag external electrodes. Therefore, development of the MPA, having superior electrical properties, a high reliability and a possibility of mass production at low cost, is required.

In this study, to manufacture the MPAs devices which have low cost and good displacement characteristics, we chose a composition of PNN–PT–PZ systems that have extensive application for commercial actuators<sup>9–12</sup> and have a low sintering temperature ( $\leq 1100^\circ\text{C}$ ), and manufactured the MPAs devices using 70Ag/30Pd paste of low cost as an internal electrode by the multilayer ceramic capacitors (MLC) techniques. Also we investigated the structural, the piezoelectric properties and the displacement characteristics of the MPA devices. Then, we appreciated the application possibilities for practical uses.

---

\* Corresponding author. Tel.: +82-2-393-3973; fax: +82-2-393-3973.

E-mail address: IHKKH@hitel.net (I.-H. Im).

## 2. Experimental

### 2.1. Preparation of multilayer actuators

The ceramic composition used in this study was  $(\text{Pb}_{0.94}\text{Ba}_{0.04}\text{Cd}_{0.02})(\text{Ni}_{1/3}\text{Nb}_{2/3})_{0.15}(\text{Zr}_{0.3}\text{Ti}_{0.7})_{0.85}\text{O}_3$ . The dielectric and piezoelectric properties measured from ceramic disk are presented in Table 1 for a reference.<sup>13</sup> The flow chart for the fabrication process of the MPA, including preparation of green sheet by a tape-casting, is given in Fig. 1. The weight ratio of ceramic powder to PVB (MSI, B73210) used as a binder was 65:35. The 70Ag/30Pd pastes (FERRO, E-1401) were printed on the green sheets using a rotary printer (Model 134, TAM) for the internal electrodes. A conventional MLC (multilayer ceramic capacitors) design was used to form the electrode configuration of the MPA as depicted in

Table 1  
Electric properties of the material used in this study

$\epsilon_{33}^T/\epsilon_0$	4500
$S_{33}^E$ ( $10^{-12}\text{m}^2/\text{N}$ )	21.4
$d_{33}$ (pC/N)	650
$k_{33}$ (%)	74.5
$T_c$ ( $^\circ\text{C}$ )	200

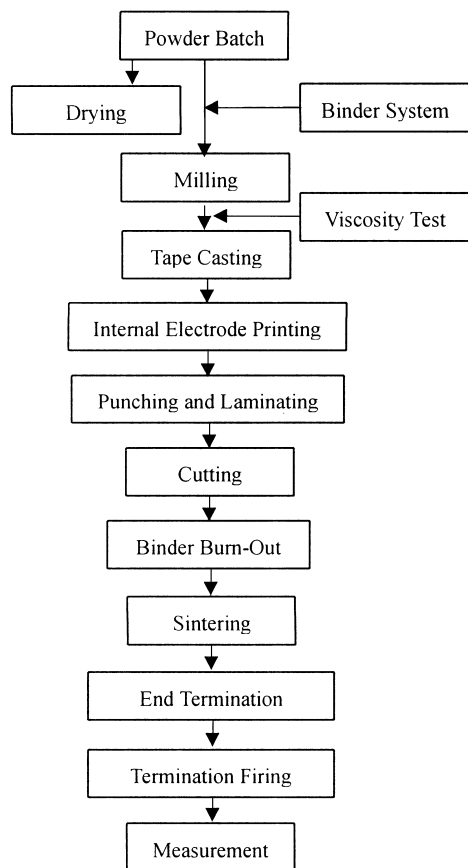


Fig. 1. Flow chart for the MPAs fabrication.

Fig. 2. The ratio of the effective internal electrode area to the cross-sectional area was designed to be 0.935 to minimize the effect of the non-active region to the MPA.<sup>6,7</sup> Green sheets printed with AgPd paste were alternatively stacked into 75 layers. The internally electroded and stacked sample was placed between two cover sheets consisting of stacking seven green sheets. Green bars ( $50\times 50\text{ mm}^2$  in size) were fabricated using a laminator (Model 109, TAM), applying a constant pressure of 3000–4000 psi at  $50^\circ\text{C}$  for 30 min. In order to minimize problems caused by shrinkage and expansion of the specimens during the binder burn-out process, binder burn-out was carried out at  $300^\circ\text{C}$  for 12 h with raising rate of  $5^\circ\text{C}/\text{h}$  and cooling rate of  $30^\circ\text{C}/\text{h}$ . The specimens were afterwards sintered at  $1050^\circ\text{C}$  for 3 h in a closed MgO crucible in air. The sintered MPA was  $8.2(\text{L})\times 5.0(\text{W})\times 3.15(\text{H})\text{ mm}^3$  in size. Ag pastes (Dupont 7095) as external electrodes were then printed as shown in Fig. 2. The MPAs were poled by applying  $30\text{ kV}/\text{cm}$  dc field at  $120^\circ\text{C}$  for 30 min.

### 2.2. Measurements

The microstructure of the MPA was observed by a scanning electron spectroscopy, SEM (JSM-6320, JEOL). Capacitance and dissipation factor of the MPA as a function of temperature were measured using a test chamber (4220A Test Chamber, S&A, Inc.). Piezoelectric properties were measured at room temperature using direct observation of strain as a function of electric field as well as low-field property measurement using the IEEE resonance technique after aging at  $100^\circ\text{C}$  for 24 h. Displacement measurements of the MPA were performed using a measurement circuit as shown in Fig. 3. A strain gauge (KFG-1-120-C1-11L1M2R, KYOWA) was attached to the MPA, parallel to the poling direction. The strain values were calculated by measuring the change of resistance of the strain gauge using a strain amplifier (DSA-692, NMB).

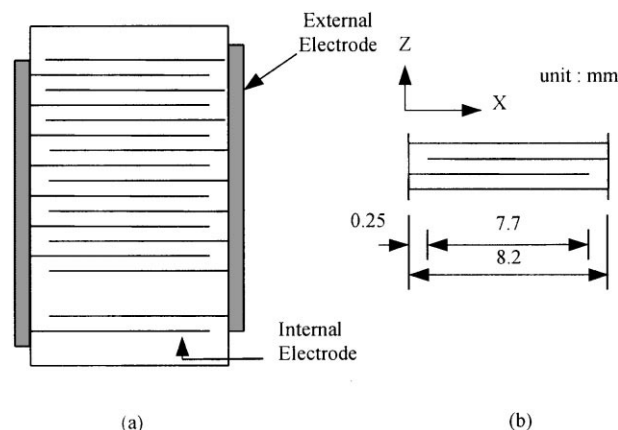


Fig. 2. (a) Cross-section and (b) dimension of the MPA.

### 3. Results and discussion

#### 3.1. Sintering characteristics

Fig. 4 and 5 present the SEM photographs of the surface and cross-section of the MPA. As shown in Fig. 4, the surface of the MPA has a grain size of 4–5  $\mu\text{m}$  and a dense structure with no open pore and agglomerated second phases. It is clearly revealed from Fig. 5 that the cofired MPA with the AgPd electrode show good sinterability without shortage of electrodes and diffusion of the internal electrode into the ceramic body.

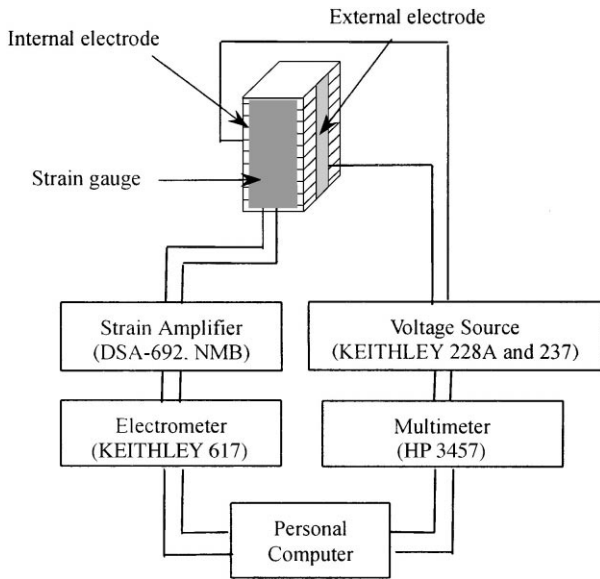


Fig. 3. Schematic diagram of strain measurement circuit.

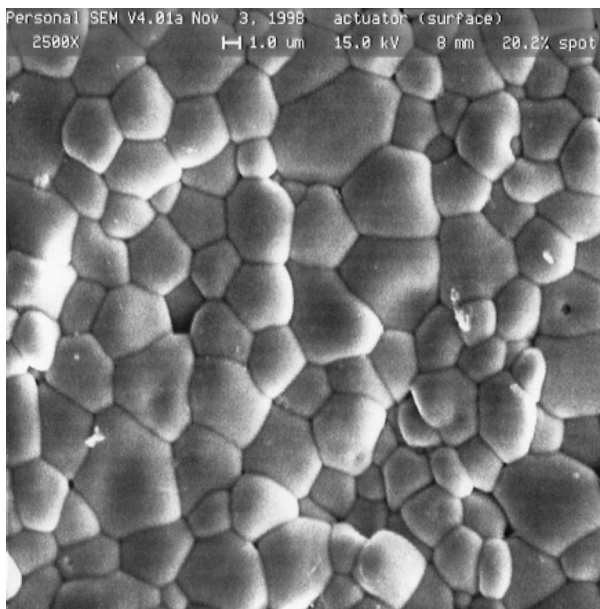


Fig. 4. SEM photograph of the MPA surface.

It is noted from the above results that the shrinkage of the internal electrode, by anti-sintering effect, was considerably reduced due to the 1–2 wt% zirconium oxide contained in the internal electrode. And also, the MPA did not exhibit the delaminations and cracks in the ceramic bodies, the gapping phenomena caused by thermal expansion coefficient difference between Pd internal electrodes and ceramics parts or protection phenomena by thermal diffusion of Ag external electrodes. Therefore, the AgPd paste showing good matchability with ceramics can be effectively adopted for the MPAs.

#### 3.2. Temperature vs capacitance characteristics

Fig. 6 presents the capacitance and the dissipation factor of the MPA as a function of temperature. As

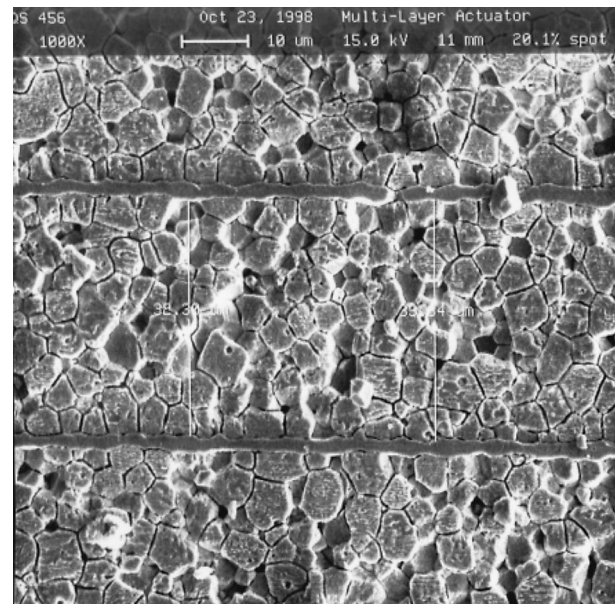


Fig. 5. SEM photograph of the cross-section of the MPA.

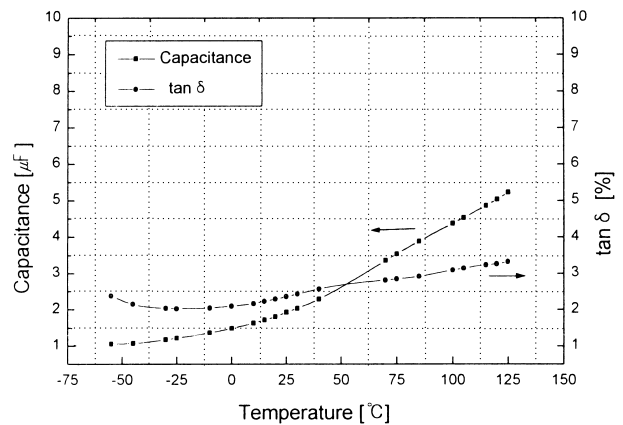


Fig. 6. Capacitance and  $\tan \delta$  characteristics of the MPA as a function of temperature.

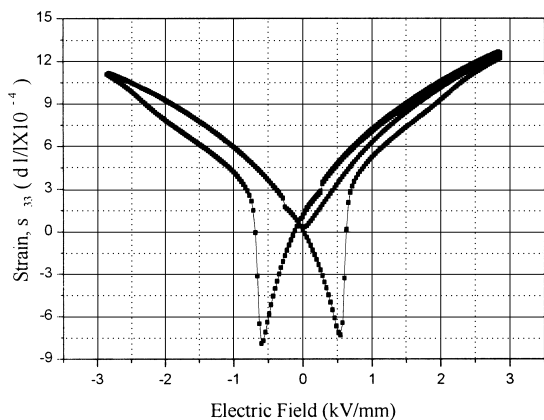


Fig. 7. Displacement characteristics of the MPA as a function of electric field.

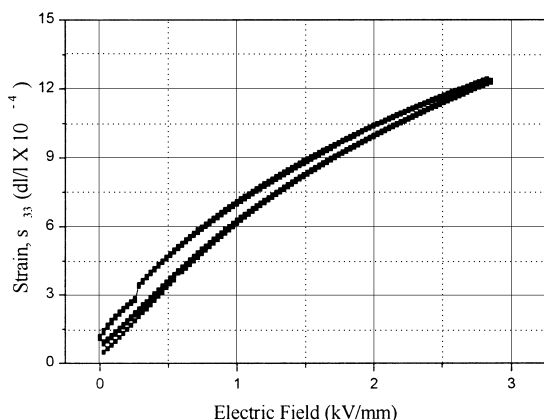


Fig. 8. Repetition characteristics of the MPA as a function of electric field.

shown in Fig. 6, the capacitance and dissipation factor of MPAs was 1.92  $\mu\text{F}$  and 2.36 [%] at room temperature.

The MPA is often fractured owing to self heat generation under dc bias since the dissipation factor of the MPA tends to increase when the adhesion and matching properties between the ceramic body and internal electrode are poor.

The dissipation factors of the MPA obtained in this study showed the values of 2.03–2.57% in the actual operating temperature range of  $-25$  to  $-75^\circ\text{C}$ . It showed equal or superior properties compared with those of the products of other companies. It means that the adhesion and combination between the ceramic body and 70Ag/30Pd paste were superior.

### 3.3. Strain vs electric field characteristics

Strain of the MPA as a function of electric field is presented in Figs. 7–9. The MPA exhibited a typical butterfly shape for ferroelectrics and maximum strain of  $4 \mu\text{m}$  at 2.85 kV/mm. The MPA prepared in this study showed the displacement characteristics of  $1.27 \mu\text{m}/100$

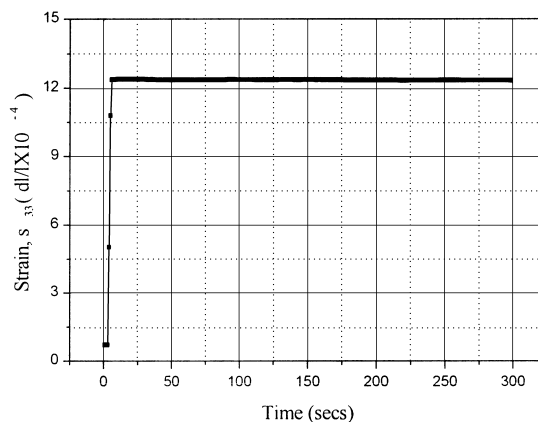


Fig. 9. Creep characteristics of the MPAs as a function of time at 100 V dc.

V-mm which is superior when compared with  $0.72 \mu\text{m}/100$  V-mm obtained from NLA-a $\times$ b $\times$ 9 series made by Tokin Co., Japan.

Fig. 8 shows repetition properties of the MPA with 3 cycles of voltage applied over a practical usage range of 0–100 V.

Fig. 9 shows time dependence of strain for the MPA under dc 100 V for 300 s. As shown in Fig. 9, the MPAs have a stable displacement property.

The creep was 0.06% by definition of  $(u_n, 30 - u_n, 01) / u_n, 01$ .<sup>14</sup>

## 4. Conclusion

Using 70Ag/30Pd paste as internal electrodes being of low cost and low sintering temperature, we fabricated the MPAs with 75 layers which have layer thicknesses of 30–35  $\mu\text{m}$ . It was clearly shown that the 70Ag/30Pd paste electrodes had a good matchability with PNN-PT-PZ ceramics, cofired at  $1050^\circ\text{C}$  for 3 h since no defects such as delamination of ceramic layers, diffusion of internal electrode into ceramic body, shortage of internal electrode and gapping phenomena were detected. The MPA exhibited maximum displacement of  $\sim 4 \mu\text{m}$  at 2.85 kV/mm, superior to other products. The dissipation factor of the MPA was below 3%, applicable to practical uses due to low heat generation. Therefore, we confirmed that the MPA having a low cost and a good electrical property can be mass-produced using a AgPd internal electrode.

## References

1. NIKKEI Mechanical, 13 June, 1988.
2. Tanaka: Bimorph shutter, Minolta Techno Report, 5, 1988.
3. NIKKEI Mechanical, 14 June, 1993.
4. Takahashi, S., Multilayer piezoelectric ceramic actuator and their application. *Jpn. J. Appl. Phys.*, 1985, **24**(Suppl. 24-2), 41.

5. Suga, M. and Tsuzuki, M., Improved drop ejection characteristics through use of micro-valves in ink jet head. *Jpn. J. Appl. Phys.*, 1984, **23**(6), 765–773.
6. Ohde, N., Utsumi, K., Ochi, A. and Takahashi, S., A multilayer piezoelectric actuator with low driving voltage. IECEJ Technical Report, CPM 88–52, 220, 7–12, 1988.
7. Takahashi, S., Ochi, A., Yonezawa, M., Yano, T., Hamatsuki, T. and Fukui, I., Internal electrode piezoelectric ceramic actuator. *Ferroelectric*, 1983, **50**, 181.
8. Takahashi, S., Ochi, A., Yonezawa, M., Yano, T., Hamatsuki, T. and Fukui, I., Internal electrode piezoelectric ceramic actuator. *Jpn. J. Appl. Phys.*, 1983, **22**( Suppl. 22-2), 157.
9. Moon, J. M. and Jang, H. M., Effect of sintering atmosphere on densification behavior and piezoelectric properties of  $\text{Pb}(\text{Ni}_{1/3}\text{Nb}_{2/3})\text{-PbTiO}_3\text{-PbZrO}_3$  ceramics. *J. Am. Ceram. Soc.*, 1993, **76**(2), 549–552.
10. Dong, D., Murakami, K., Kaneko, S. and Xiong, M., Piezoelectric properties of PZT ceramics sintered at low temperature with complex-oxide additives. *J. Ceram. Soc. Jpn.*, 1993, **101**(10), 1090–1094.
11. Moon, J. M. and Jang, H. M., Densification and piezoelectric properties of  $\text{MnO}_2$ ,  $\text{SiO}_2$  doped  $\text{Pb}(\text{Ni}_{1/3}\text{Nb}_{2/3})\text{-PbTiO}_3\text{-PbZrO}_3$  ceramics. *J. Mater. Res.*, 1993, **8**(12), 3184–3191.
12. Zhilum, G., Longtu, L., Hongqung, L. and Xiaowen, Z., Low temperature sintering of lead magnesium nickel niobate zirconate titanate (PMN–PNN–PZT) piezoelectric ceramics, with high performances. *Ferroelectrics*, 1990, **101**, 93–99.
13. Cho, C. H., Park, I. K., Kim, H. G. and Chung, H. T., Sintering behavior of cadmium-doped  $\text{Pb}(\text{Ni}_{1/3}\text{Nb}_{2/3})\text{-PbTiO}_3\text{-PbZrO}_3$  ceramics. *J. Am. Ceram. Soc.*, 1997, **80**(6), 1523–1534.
14. Uchino, K. *Piezoelectric Actuators and Ultrasonics Motors*. Kluwer Academic Publishers, Appendices, 1997, p. 336.